Applied Physics A (2019) 125:628
https://doi.org/10.1007/s00339-019-2925-x

Applied Physics A
Materials Science & Processing

A compact dual band antenna based on metamaterial-inspired split ring structure and hexagonal complementary split-ring resonator for ISM/WiMAX/WLAN applications

B. Murugeshwari[1] · R. Samson Daniel[1] · S. Raghavan[2]

Received: 2 March 2019 / Accepted: 9 August 2019 / Published online: 16 August 2019

Abstract

A miniaturized dual-band antenna is proposed for industrial scientific and medical (ISM), worldwide interoperability for microwave access (WiMAX), and wireless local area network (WLAN) applications. The proposed antenna consists of hexagonal complementary split-ring resonator (HCSRR), metamaterial-inspired split-ring structure, and a partial ground plane. The prototype antenna is fed by 50-Ω microstrip feed line, which is printed on a $30 \times 30 \times 0.8$ mm^3 FR-4 substrate. HCSRR in the radiating element is used to create a new resonance at 2.4 GHz for achieving dual-band characteristics. A split in the outer hexagonal ring induces a magnetic resonance which leads to improvement of the bandwidth of the antenna. The proposed antenna is fabricated and measured. The measured -10-dB impedance bandwidths are 180 MHz (2.42–2.60 GHz) and 2400 MHz (3.44–5.84 GHz) with a resonance frequency of 2.56 GHz and 4.64 GHz, respectively, which is suitable for ISM, WiMAX, and WLAN applications. Analysis of HCSRR is discussed in detail using empirical design equation with metamaterial property. The prototype antenna has suitable radiation characteristics for all resonance frequencies.

1 Introduction

The design of dual-band antenna with broad bandwidth is very much desirable to cover all the specified frequencies. This technique can be used to replace many antennas by single antenna. Numerous techniques have been investigated to achieve dual-band antenna design. Rectangular notch [1], loop structure [2], embedding slot [3], and parasitic element [4] in the radiating patch are few among them to realize dual-band antenna. Recently electromagnetic (EM) metamaterial has got great attention in antenna design for enhancing the antenna performances.

Metamaterial offers negative values of permeability (μ) and permittivity (ε) from its basic elements such as split-ring resonator (SRR) and its dual element (CSRR). These unique properties are not found in natural materials. Metamaterial-inspired split ring, SRR and CSRR, structures have been used as radiating elements for improving antenna radiation characteristics [5–11]. Inscription of metamaterial-inspired split-ring structure has been investigated in attaining multiband antenna due to band notch characteristics [12] and reconfigurability [13]. Negative refractive index-transmission line (NRI-TL) [14, 15] satisfies the metamaterial properties due to its series capacitance and shunt inductance for designing broad-bandwidth antenna. Large number of researchers have concentrated on split-ring structure for achieving bandwidth improvement.

In this paper, a miniaturized dual-band antenna based on the metamaterial-inspired split ring and HCSRR is proposed for ISM/WiMAX/WLAN (2.4/3.5/5.5 GHz) applications. HCSRR is capable of creating new resonance frequency of 2.4 GHz. The split in the ring element induces a time-varying magnetic field and in turn used to create a broad bandwidth. The metamaterial characteristics of HCSRR are verified for achieving a lower resonance frequency to realize antenna miniaturization. A good mechanism is used to cover dual band and bandwidth enhancement without altering the size of the antenna.

✉ B. Murugeshwari
bmwinece@gmail.com

1 Department of Electronics and Communication Engineering, K. Ramakrishnan College of Engineering, Samayapuram, India

2 National Institute of Technology, Tiruchirappalli 620015, India

2 Antenna design and principle of operation

The design steps of the prototype antenna are described in Fig. 1. Configuration A shows a hexagonal ring radiating element. The resonance frequency of ring radiating element is calculated by [5]

$$f_r = \frac{1.8412 \times c}{2\pi S\sqrt{\varepsilon_r}} = \frac{1.8412 \times 3 \times 10^8}{2 \times \pi \times 12 \times 10^{-3} \times \sqrt{4.4}} = 3.5 \text{ GHz} \tag{1}$$

here, S is the side length of the hexagonal ring radiating element and ε_r is the dielectric constant of the FR-4 substrate. Therefore, the antenna resonates at 3.5 GHz for a side length of 12 mm. In configuration B, a small hexagonal patch is introduced. The metallic stub is used to connect hexagonal ring radiating element and hexagonal patch. The stub is used to couple the electromagnetic energy from the hexagonal ring to hexagonal patch. After that, HCSRR is embedded at the distance (d_1) of 11.05 mm ($\lambda_g/5.71$) from the bottom of the feed position. It changes the current path of patch antenna and in turn creates dual-band characteristics. In the next step, to achieve wider bandwidth, a split is created in the horizontal arm of the outer hexagonal ring as shown in configuration C.

The layout of the proposed antenna along its side view is shown in Fig. 2, and dimensions are listed in Table 1. The snapshot of the fabricated antenna is shown in Fig. 3.

The simulations are carried out using finite element method (FEM)-based Ansoft high-frequency structure simulator (HFSS) V.15.0 software. The comparison of the reflection coefficient of the antenna with three different configurations is shown in Fig. 4. It depicts that, configuration A has a single-band resonance around 3.5 GHz with a wider impedance bandwidth of 3190 MHz (2.82–6.01 GHz). When the HCSRR is introduced (configuration B), dual-band characteristics have been observed. The first band has a resonance frequency of 2.4 GHz with an impedance bandwidth of 180 MHz (2.32–2.50 GHz) and the second band has dual resonance of 4.07 GHz and 4.8 GHz with an impedance bandwidth of 2230 MHz (3.13–5.36 GHz). In configuration C (proposed antenna), a split is embedded in the horizontal arm of the outer hexagonal ring. Now, the impedance bandwidth of second band has been improved without affecting the first band. Also, it is found that there is a shift in resonant frequency of 4.8–5.25 GHz due to its capacitance effect of the split ring.

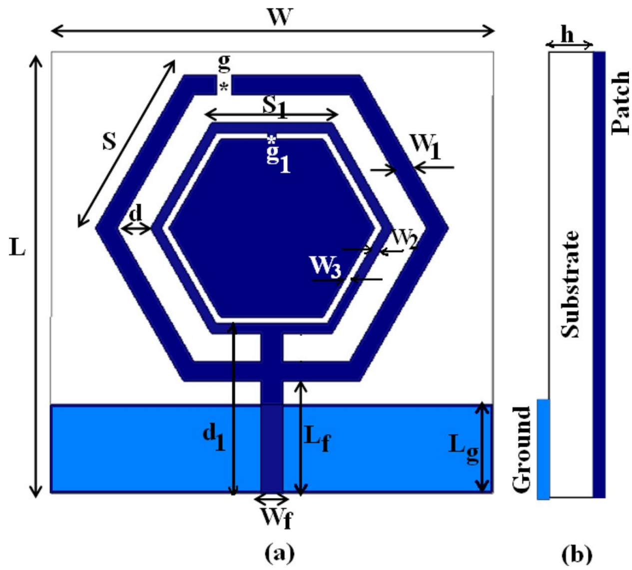

Fig. 2 Geometry of the proposed antenna. **a** Top view and **b** side view

The proposed antenna exhibits dual-band characteristics. The first band has a resonance frequency of 2.4 GHz with an impedance bandwidth of 180 MHz (2.32–2.50 GHz) and the second band has dual resonance of 4.07 GHz and 5.25 GHz with an impedance bandwidth of 2610 MHz (3.13–5.74 GHz).

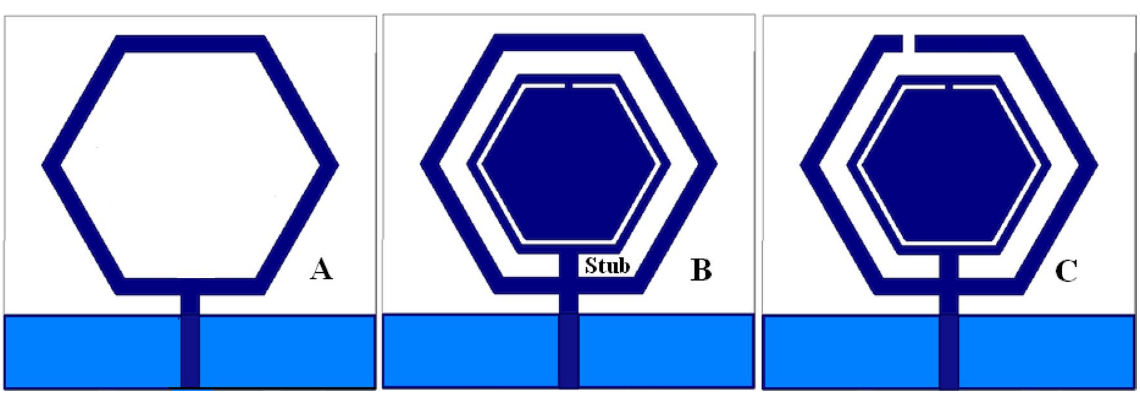

Fig. 1 Evolution stages of prototype antenna

Table 1 Parameters of the prototype antenna

Parameter	Dimension (mm)
W	30
L	30
W_f	1.5
L_f	7.6
S	12
S_1	8.25
L_g	6
d	2.25
g	1
g_1	0.5
W_1	1.5
W_2	0.5
W_3	0.5

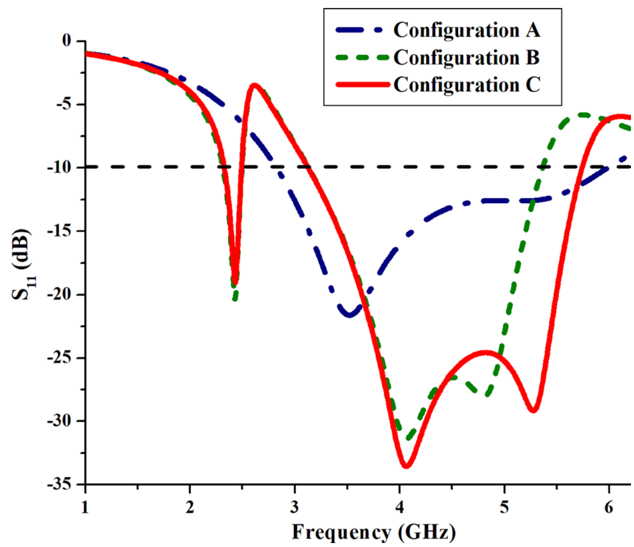

Fig. 4 Reflection coefficient of the antenna with three different configurations

3 Parametric study

Parametric investigation is done on the reflection coefficient of the proposed antenna for various ground plane lengths (L_g), the width of the hexagonal ring (W_1), and width of the feed line (W_f) to achieve the optimum dimensions of the antenna. The ground plane length (L_g) is varied from 4.5 to 6 mm and width of the hexagonal ring (W_1) is varied from 3 to 1.5 mm with incremental step of 0.5 mm, which are shown in Figs. 5 and 6, respectively. It is found that wider bandwidth is observed for $L_g = 6$ mm and $W_1 = 1.5$ mm.

Similarly, reflection coefficient of the microstrip feed width (W_f) is shown in Fig. 7. The width (W_f) creates an essential role for determining impedance matching (50 Ω) of the antenna, which is varied from 0.9 to 1.7 mm in steps of 0.2 mm. It is inferred that, as the width of the microstrip feed (W_f) increases, the impedance matching of second band is affected more compared with first band. However, the optimum performance of

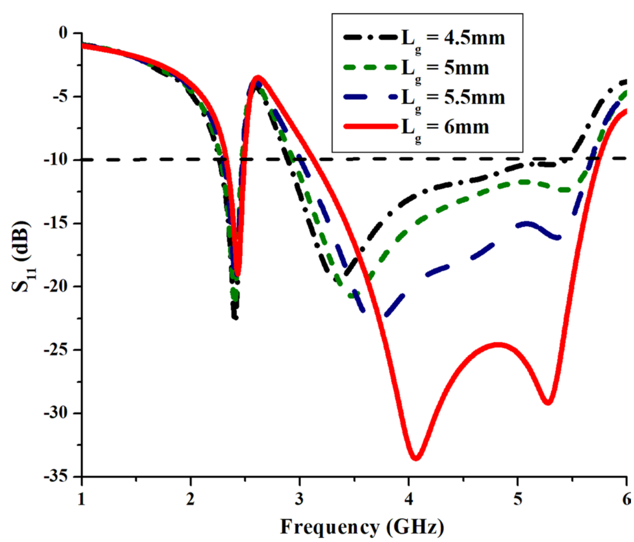

Fig. 5 Reflection coefficient of the antenna for variation of L_g

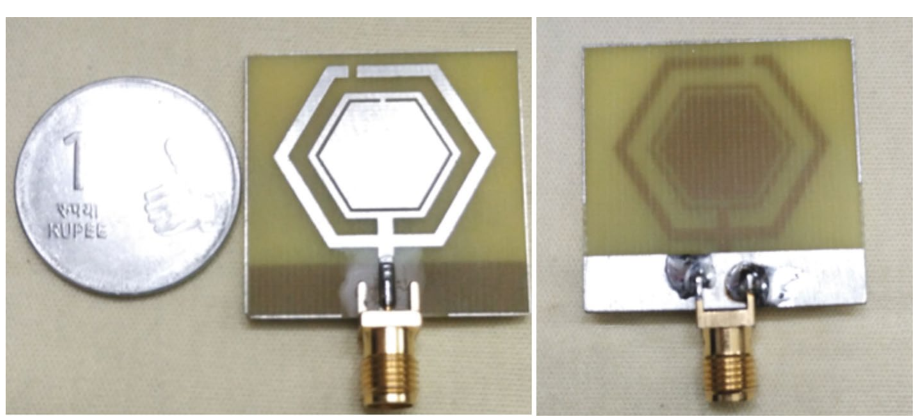

Fig. 3 Photograph of the fabricated proposed antenna (top view and bottom view)

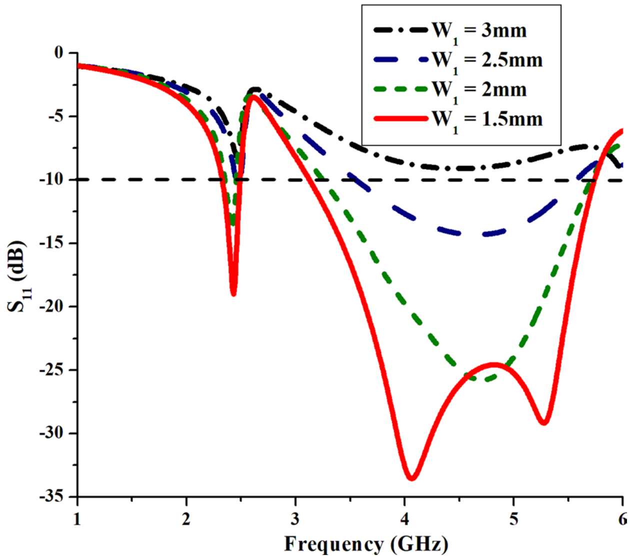

Fig. 6 Reflection coefficient of the various width (W_1) of the hexagonal ring

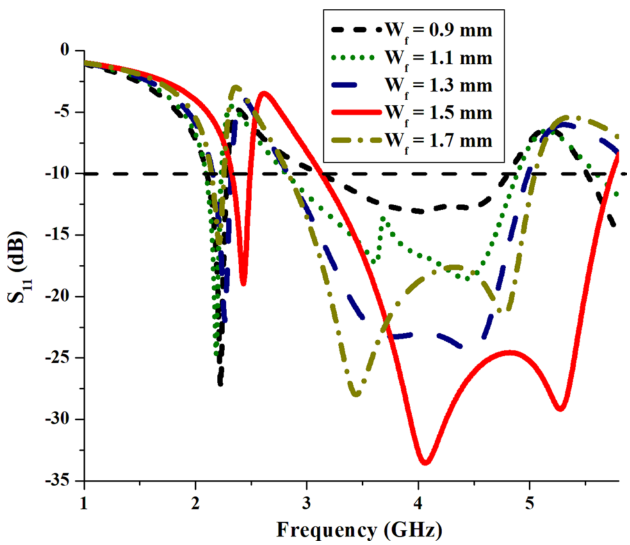

Fig. 7 Reflection coefficient of the antenna with variation of W_f

the antenna is obtained for $W_f = 1.5$ mm. Hence, based on the parametric study, dimensions are chosen for fabrication.

The evaluation of prototype antenna with other metamaterial antennas is listed in Table 2. From Table 2, it is perceived that the prototype antenna covers dual band for ISM, WiMAX, and WLAN applications with compact size. This paper highlights the equivalent circuit analysis of HCSRR and the evidence of metamaterial property (negative permittivity) for generating a new resonance frequency. The antennas listed in reference failed to study metamaterial property.

4 Equivalent circuit analysis of HCSRR

HCSRR creates a new resonance frequency of 2.4 GHz, which is examined by LC equivalent circuit model [16], as illustrated in Fig. 8. The metal slit between the HCSRR slot is essential for constructing passband characteristics. HCSRR slot produces the capacitance effect $\left(C_{HCSRR}\right)$ and metal slit between the HCSRR slot produces an inductance effect $\left(L_{HCSRR}\right)$. Therefore, the resonance frequency of HCSRR $\left(f_{HCSRR}\right)$ is evaluated by [17]

$$f_{CSRR} = \frac{1}{2\pi\sqrt{L_{CSRR}C_{CSRR}}}, \tag{2}$$

$$C_{CSRR} = \frac{N-1}{2}[2L - (2N-1)(W+S)]C_0,$$

$$C_0 = \varepsilon_0 \frac{K\left(\sqrt{1-K^2}\right)}{K(k)} \text{ and } k = \frac{S/2}{W + S/2},$$

$$L_{CSRR} = 4\mu_0[L - (N-1)(S+W)]\left[\ln\left(\frac{0.98}{\rho}\right) + 1.84\rho\right]$$

$$\rho = \frac{(N-1)(W+S)}{1-(N-1)(W+S)}.$$

Table 2 Comparison of other metamaterial antennas

References	Year	Patch detail	Dimensions $L \times W$ (mm^2)	Frequency (GHz)	Metamaterial property verification
[6]	2011	Triangular SRR	40 × 35	1.96–4.33, and 5.05–7.32	Not verified
[7]	2013	Truncated square patch and split-ring resonator	66.4 × 66.4	0.68, 1.33, and 1.41	Not verified
[8]	2013	Rectangular patch and CSRR	34 × 30	2.3–2.6, 3.3–3.7, and 5.1–5.5	Not verified
[9]	2014	Slot antenna and split-ring resonator	50 × 40	1.65, 1.93, and 2.20	Not verified
[10]	2015	Slot, rectangular patch, and metamaterial unit cells	45 × 40	2.3–4, and 5–6.6	Not verified
[11]	2016	Inverted-L and split ring resonators	40 × 70	1.54, 1.63, 2.25, and 3.69	Not verified
Proposed			30 × 30	2.32–2.50, and 3.13–5.74	Verified

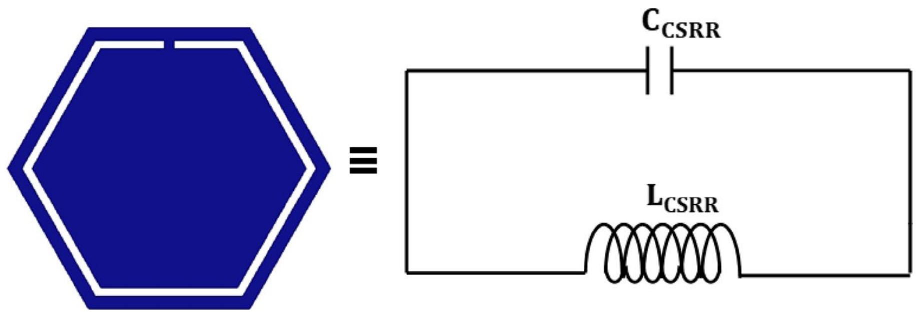

Fig. 8 HCSRR and its equivalent circuit model

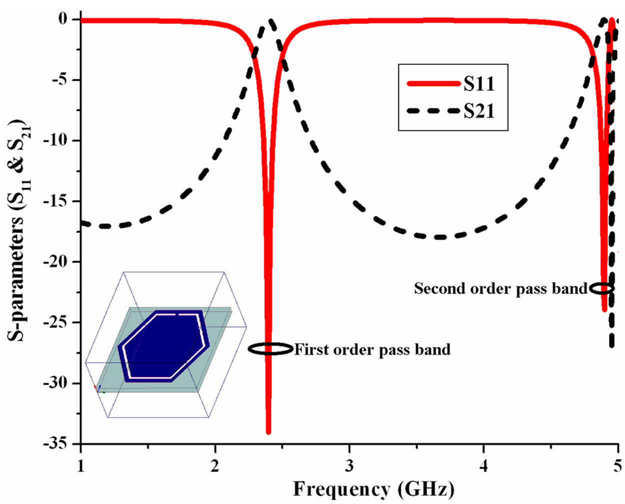

Fig. 9 Simulated S-parameters $\left(S_{11} \text{and} S_{21}\right)$ of HCSRR

Here, L is the HCSRR side length, slot width $(W)=0.5$ mm, slit width $(S)=0.5$ mm, number of HCSRR (N) and K is the elliptic integral $K(k)$. These empirical equations are evaluated by MATLAB program to compute the HCSRR resonance frequency due to capacitance (C_{HCSRR}) and inductance (L_{HCSRR}) values.

For side length of HCSRR $(L)=7.5$ mm.

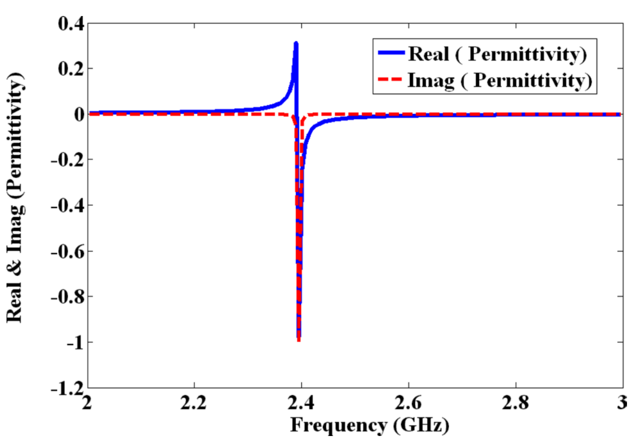

Fig. 10 Negative permittivity characteristics of HCSRR

Thus, $C_{HCSRR} = 7.5476 \times 10^{-14}$ (Farad) and $L_{HCSRR} = 5.8537 \times 10^{-08}$ (Henry). Therefore, the proposed HCSRR resonance frequency is $f_{HCSRR} = \frac{1}{2\pi\sqrt{C_{HCSRR}L_{HCSRR}}} = 2.4$ GHz.

From this LC equivalent circuit investigation, it is observed that the proposed HCSRR generates the resonance frequency of 2.4 GHz. It matches with a simulated resonance frequency of the proposed HCSRR.

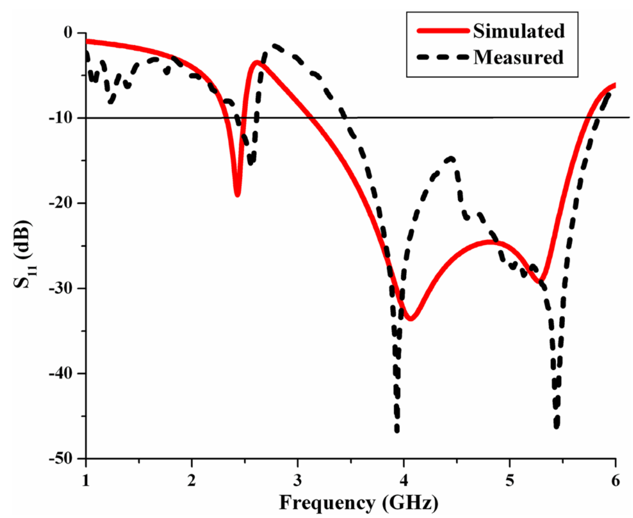

Fig. 11 Simulated and measured S_{11}(dB) of the proposed antenna

Table 3 Comparison of measured and simulated results

Proposed antenna	Band details	Resonant frequency (GHz)	Bandwidth (MHz)
Simulated	First band	2.4	180
	Second band dual resonance	4.07 and 5.25	2610
Measured	First band	2.56	180
	Second band dual resonance	3.93 and 5.44	2400

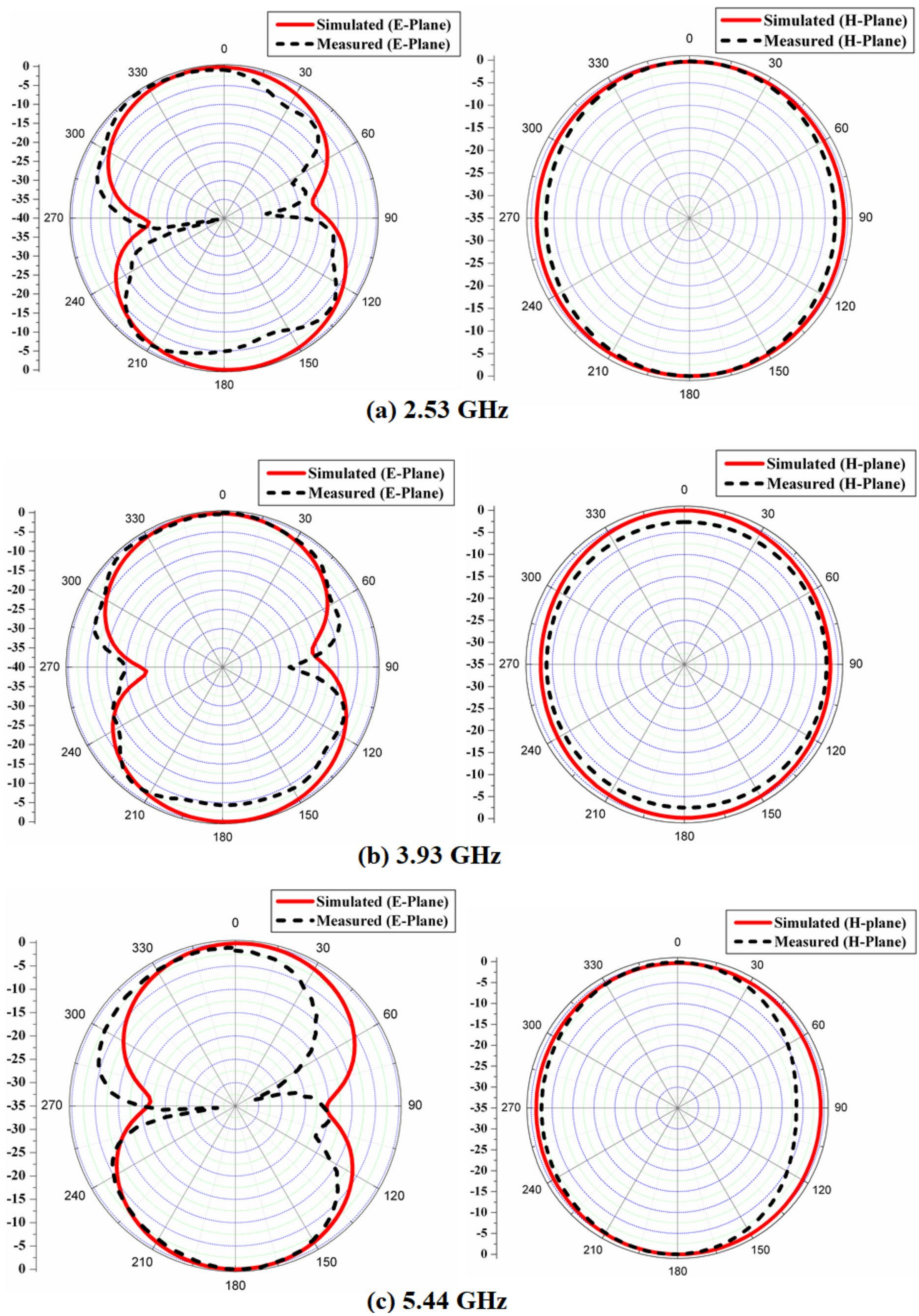

Fig. 12 Radiation pattern of proposed antenna. **a** 2.54 GHz, **b** 3.93 GHz, and **c** 5.44 GHz

5 HCSRR analysis

The band characteristics of HCSRR are analyzed using the waveguide setup [18]. The reflection coefficient $\left(S_{11}\right)$ creates a passband behavior for generating a new resonance frequency and transmission coefficient $\left(S_{21}\right)$ creates a stopband for notch characteristics [19]. The S-parameters S_{11} and S_{21} of HCSRR are extracted and compared as shown in Fig. 9. It depicts the two passband $\left(S_{11}\right)$ characteristics at 2.4 GHz and 4.8 GHz. Here, 2.4 GHz verifies to the equivalent circuit design equation of $f_{\mathrm{HCSRR}}=\frac{1}{2\pi\sqrt{C_{\mathrm{HCSRR}}L_{\mathrm{HCSRR}}}}$. Thus, it allocates the lower order mode, explained to be f_0. Also, the higher order mode is obtained at $2f_0$, as defined in [1]. The lower order mode is a unique consideration, because it confirms with the HCSRR resonance frequency of 2.4 GHz.

The extracted negative permittivity (ε) of the HCSRR is depicted in Fig. 10. It illustrates that the permittivity (ε) value at 2.4 GHz is negative due to lower order $\left(f_0\right)$ mode of HCSRR. From this S-parameter extraction, it is agreed that negative permittivity offers a new resonance frequency. Thus, the proposed HCSRR with optimized parameters has contributed a new resonance frequency of 2.4 GHz for achieving dual band antenna.

6 Results and discussion

Figure 11 shows the simulated and measured S_{11}(dB) of the proposed antenna. Both results coincide with each other. The measured data show dual-band characteristics. The first band has a resonance frequency of 2.56 GHz, and the second band has a dual resonance of 3.93 GHz and 5.44 GHz. The measured result covers -10 dB impedance bandwidth of 180 MHz (2.43–2.61 GHz) and 2400 MHz (3.43–5.83 GHz) which is useful for ISM and WLAN frequency bands. The performance evaluations of measured and simulated values are listed in Table 3.

The measured E-plane $\left(\phi = 90^{\circ}\right)$ and H-plane $\left(\phi = 0^{\circ}\right)$ radiation patterns of the proposed antenna compared with simulated radiation pattern is exposed in Fig. 12. It illustrates that the prototype antenna covers the desired directions at the resonance frequencies of 2.53 GHz, 3.93 GHz, and 5.44 GHz. The measured peak gains of the prototype antenna are shown in Fig. 13. The peak gains 0.66 dBi, 1.64 dBi, and 1.72 are inferred at 2.53 GHz, 3.93 GHz, and 5.44 GHz, respectively.

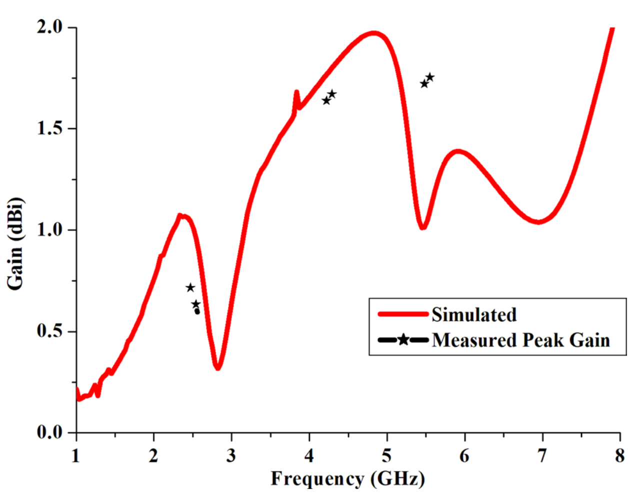

Fig. 13 Gain of the prototype antenna

7 Conclusion

The metamaterial-based monopole antenna is developed and validated on a $30\times30\times0.8$ mm^3 FR-4 substrate. In the proposed design, a HCSRR is nested with inner monopole and split is introduced on the outer horizontal arm for the radiation. The negative permittivity characteristics of HCSRR at 2.4 GHz have been examined with passband behavior. The proposed antenna has tiny size, homogeneous radiation pattern, and wider bandwidth, which is applicable for ISM and WLAN wireless applications. The simulated results are endorsed with the measured results.

References

1. W.C. Liu, C.M. Wu, Broad band dual frequency CPW-fed planar monopole antenna with rectangular notch. Electron. Lett. **40**, 1 (2004)
2. L. Qu, R. Zhang, H.H. Kim, H. Kim, Compact dual-band antenna using inverted-L loop and inner rectangular loop for WLAN applications. Electron. Lett. **51**(2015), 1844 (1843)
3. X.Q. Zhu, Y.X. Guo, W. Wu, A novel dual-band antenna for wireless communication applications. IEEE Antennas Wirel. Propag. Lett. **15**, 516–519 (2016)
4. J.L. Buckley, K.G. McCarthy, L. Loizou, B. O'Flynn, C. O'Mathuna, A dual-ISM-band antenna of small size using a spiral structure with parasitic element. IEEE Antennas Wirel. Propag. Lett. **15**, 630–633 (2016)
5. R. Samson Daniel, R. Pandeeswari, S. Raghavan, Dual-band monopole antenna loaded with ELC metamaterial resonator for WiMAX and WLAN applications. Appl. Phys. A **124**, 570 (2018)
6. K. Yang, H. Wang, Z. Lei, Y. Xie, H. Lai, CPW-fed slot antenna with triangular SRR terminated feedline for WLAN/WiMAX applications. Electron. Lett. **47**, 1 (2011)
7. S.K. Patel, Y. Kosta, Investigation on radiation improvement of corner truncated triband square microstrip patch antenna with double negative material. J. Electromagn. Waves Appl. **27**, 819–833 (2013)
8. S.C. Basaran, U. Olgun, K. Sertel, Multiband monopole antenna with complementary split ring resonators for WLAN and WiMAX applications. Electron. Lett. **49**, 636–638 (2013)
9. D. Sarkar, K. Saurav, K.V. Srivastava, Multiband microstrip fed slot antenna loaded with split ring resonator. Electron. Lett. **50**, 1498–1500 (2014)

10. H. Huang, Y. Liu, S. Zhang, S. Gong, Multiband metamaterial-loaded monopole antenna for WLAN/WiMAX applications. IEEE Antennas Wirel. Propag. Lett. **14**, 662–665 (2015)
11. S. Dakhil, H. Rmili, J.M. Floch, R.W. Ziolkowski, Printed multi-band metamaterial inspired antenna. Microw. Opt. Tech. Lett. **58**, 1281–1289 (2016)
12. S. Immaculate Rosaline, S. Raghavan, Design of split ring antennas for WLAN and WiMAX applications. Microw. Opt. Tech. Lett. **58**, 2117–2122 (2016)
13. V. Rajeshkumar, S. Raghavan, A compact reconfigurable split ring monopole antenna for WLAN/WAVE applications. Appl. Comput. Electromagn. Soc. J. **30**, 338–344 (2015)
14. Marco A. Antoniades, George V. Eleftheriades, A broadband dual-mode monopole antenna using NRI-TL metamaterial loading. IEEE Antennas Wirel. Propag. Lett. **8**(258), 261 (2009)
15. Yan Li, Quanyuan Feng, A compact tri-band monopole antenna with metamaterial loaded for WLAN/WiMAX applications. J. Electromagn. Waves Appl. **27**(772), 782 (2013)
16. R. Samson Daniel, R. Pandeeswari, S. Raghavan, A miniaturized printed monopole antenna loaded with hexagonal complementary split ring resonators for multiband operations. Int. J. RF Microw. Comput. Aid. Eng. **28**, 1–8 (2018)
17. R. Samson Daniel, R. Pandeeswari, S. Raghavan, A compact metamaterial loaded monopole antenna with offset-fed microstrip line for wireless applications. AEU Int. J. Electron. C **83**, 88–94 (2018)
18. R. Samson Daniel, R. Pandeeswari, S. Raghavan, Offset-fed complementary split ring resonators loaded monopole antenna for multiband operations. AEU Int. J. Electron. C **78**, 72–78 (2017)
19. R. Samson Daniel, R. Pandeeswari, S. Deivalakshmi, A CPW-fed dual band antenna based on metamaterial inspired split ring structure. In: IEEE International Conference on Signal and Image Processing (ICSIP), pp. 437–440 (2017)
20. R. Samson Daniel, R. Pandeeswari, S. Raghavan, Multiband monopole antenna loaded with complementary split ring resonator and C-shaped slots. AEU Int. J. Electron. C **75**, 8–14 (2017)